INTERNATIONAL JOURNAL OF PRECISION ENGINEERING AND MANUFACTURING Vol. 17, No. 5, pp. 623-629 MAY 2016 / 623
DOI: 10.1007/s12541-016-0075-z ISSN 2234-7593 (Print) / ISSN 2005-4602 (Online)

Shifting Process Control for Two-Speed Automated Mechanical Transmission of Pure Electric Vehicles

Da-Tong Qin[1,#], Ming-Yao Yao[1], Shu-Jiang Chen[1], and Sung-Ki Lyu[2]

1 State Key Laboratory of Mechanical Transmission, Chongqing University, Chongqing, 400044, China
2 School of Mechanical and Aerospace Engineering, ReCAPT, Gyeongsang National University, 501, Jinju-daero, Jinju-si, Gyeongsangnam-do, 52828, South Korea
Corresponding Author / E-mail: dtqin@cqu.edu.cn, TEL: +86-23-6510-4217, FAX: +86-23-6510-4217

KEYWORDS: Two-speed automated mechanical transmission, Clutchless AMT, Electric vehicle, Shifting process, Parallel coordination control

Shifting processes are analyzed for a pure electric vehicle equipped with a two-speed automated mechanical transmission without a clutch in order to study the relationship between shifting jerk, shifting time, and synchronizer tooth grinding. Results show that shifting time has a negative correlation with shifting jerk, which is related to the torque variation rates of the driving and shifting motors. Tooth grinding of the synchronizer is related to the relative speed between the synchronizer sleeve and lock ring during shifting processes. Based on the analysis, a shifting control strategy for pure electric vehicles is proposed in order to decrease shifting jerk, avoid tooth grinding of the synchronizer, and shorten shifting time. Experimental results obtained show that the proposed control strategy can achieve smooth, reliable, and quick shifts for an electric vehicle.

Manuscript received: March 31, 2015 / Revised: December 23, 2015 / Accepted: January 4, 2016

1. Introduction

Electric vehicles (EVs) are an attractive and promising solution to the issues of pollution and petroleum shortage that result from conventional gasoline-powered vehicles.[1,2] In order to minimize the cost and drivetrain mass of the gearbox, EVs are usually equipped with a single-speed gearbox.[3] To improve the dynamic and economic performance of EVs, the drive systems of a pure electric vehicle are modified from fixed-ratio drive systems to variable-ratio drive systems.[4-8] An automated mechanical transmission (AMT) has the advantage of higher efficiency and lower production cost compared with conventional manual transmission (MT);[9,10] therefore, AMT is considered an ideal transmission type for pure electric vehicles.

The coordinated control of the engine and clutch is the focus of AMT shifting process control research in present investigations. The inertia of the motor is significantly diminished compared to that of the engine; thus, clutchless AMT becomes more feasible for EVs, especially in terms of cost reduction. The AMT without clutch can be classified into two types: the power continuation type represented by the Zeroshift, and the power interruption type represented by the clutchless AMT.

Zeroshift[11,12] utilizes two sliding blocks to realize no power interruption shifting, which is different from the conventional AMT. This can be considered an improved method for the synchronizer. Zeroshift is more suitable for multi-gear transmission because the rotational speed difference between the two adjacent gears is not apparent. When considering power performance, 2 or 3 transmission gears are enough for EVs,[13] and the rotational speed difference between the two adjacent gears is in the range of 2000 to 3000, or even greater. The buffer device (spring) is used to solve the problem of rotational speed difference during shifting for Zeroshift. If the rotational speed difference is too large to be buffered, the input shaft may be locked and the output shaft may be suffering from a loss of power. For the sake of safety and ride comfort, Zeroshift should not be adopted for EVs with 2 or 3 transmission gears.

The clutchless AMT can be understood as a traditional AMT removing the clutch. The control shifting strategy was studied for the traditional engine vehicle equipped a clutchless AMT, and it has been found that shifting of a clutchless AMT could be achieved by controlling torque and speed of the engine and movement of shifting motor. It proves the feasibility of clutchless AMT equipped onto vehicles.[14-17] Compared to those of the engine, the driving motor torque and speed can be controlled more easily, therefore, the clutchless AMT is more suitable for EVs. Practical tests show that long shifting time and synchronizer tooth grinding are the main issues in the shifting process. Wang Y. investigated the mechanism of synchronizer tooth grinding and proposed a shifting process control strategy that prevents synchronizer

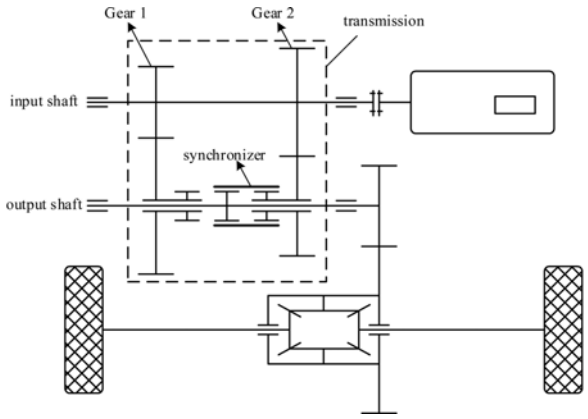

Fig. 1 Structural diagram of a clutchless two-speed AMT

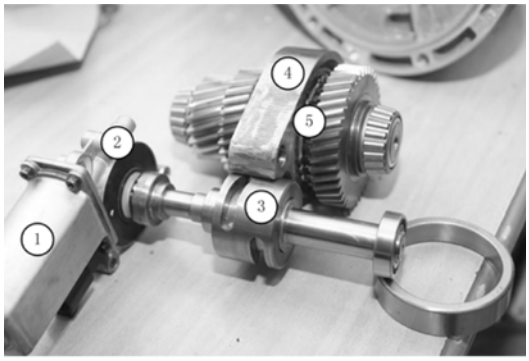

1-Shifting motor; 2-Worm gear mechanism; 3-Shifting cam; 4-Shifting fork; 5-Synchronizer

Fig. 2 Shifting actuator structure

tooth grinding by reducing the synchronizer axial movement speed, but at the expense of shifting time.[18] Chen Y. D. proposed a shifting process control strategy for pure electric vehicles equipped with AMT to solve the issue of downshifting difficulty.[19] In his strategy, the target speed of the driving motor is set higher than the theoretical speed in order for the synchronous and friction torques to be in the same direction, thus decreasing the shifting time. However, in the aforementioned strategy, the tooth grinding issue of the synchronizer was not taken into consideration.

In this paper, the issues of long shifting time and tooth grinding are investigated for a pure electric vehicle equipped with a two-speed clutchless AMT. In order to realize smooth, reliable, and quick shifts, the shifting process is analyzed quantitatively. The causes of long shifting time and synchronizer tooth grinding are studied, and the shifting control strategy for pure electric vehicles is developed based on the parallel coordination control method. A shifting experiment is also carried out. The prospective goal is achieved in the experiment, demonstrating a good practical result of the clutchless two-speed AMT that may be useful for future applications.

2. Shifting Process

A structural diagram of the two-speed clutchless AMT of a pure electric vehicle is shown in Fig. 1.[20] The two-speed AMT without a clutch adopts an electronically controlled motor driving system that is composed of a shifting motor, a worm gear reducer, a shifting cam, a shifting fork, and a synchronizer. The synchronizer is the same as the one used in regular MT and is installed on the output shaft as shown in Fig. 2. The shifting groove in the shifting cam is used to convert the rotational motion of the shifting cam into the axial motion of the shifting fork, in order to achieve the functions of gear disengaging and engaging, as shown in Fig. 3.

In Fig. 3, θ_1 represents the area of Gear 1, θ_2 represents the area of Gear 2, θ_N represents the neutral Gear area, $\theta_{1\text{-}N}$ is the 1-N transition area, and $\theta_{2\text{-}N}$ is the 2-N transition area. As shown in Fig. 3, the rotational motion of the shifting cam will not be converted into the axial motion of the shifting fork in Gear 1, Gear 2, and neutral Gear areas. However, the rotational motion of the shifting cam will be converted into the

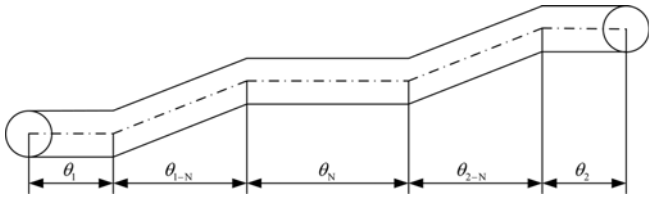

Fig. 3 Expansion plan of the shifting groove on cam

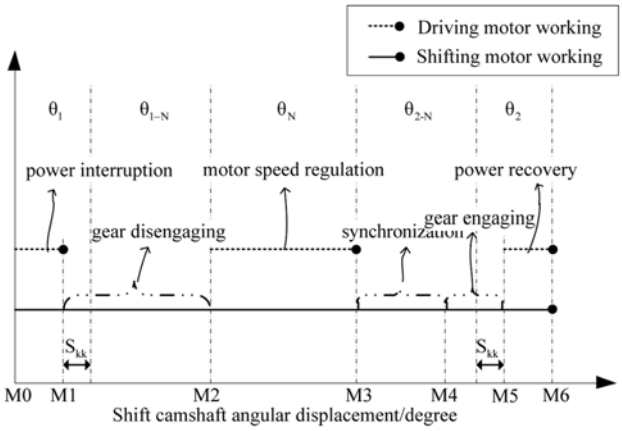

Fig. 4 Shifting process diagram

axial motion of the shifting fork in the transition area between Gear 1 and neutral Gear areas, or in the transition area between the neutral Gear and Gear 2 areas.

The shifting process of a clutchless AMT involves the complex coordination control process of the shifting and driving motors. It usually adopts the serial coordinated control method for the shifting and driving motors. That is, the shifting and driving motors are alternately controlled in the shifting process. According to the serial coordination control method, the shifting process can be divided into 6 stages: (1) power interruption, (2) gear disengaging, (3) motor speed regulation, (4) synchronization, (5) gear engaging, and (6) power recovery.

As described above, the rotation of the shifting camshaft will not

cause axial movement of the synchronizer sleeve when the two-speed AMT is in Gear 1, Gear 2, or neutral Gear areas. On the basis of this characteristic, a parallel coordination control method for the shifting and driving motors is proposed in order to shorten the shifting time. Just like serial coordination control, the parallel coordination control strategy can also be divided into 6 stages. However, unlike serial control, the shifting motor is always working during the shifting process (as shown in Fig. 4).

In Fig. 4, it must be noted that S_{kk} represents a stroke that guarantees the upshifting or downshifting operation. If the shifting fork is in the M1-M5 stage, then the gear is not on the Gear and the torque cannot be well transmitted through the AMT. In other words, in the stages of power interruption (M0-M1) and power recovery (M5-M6), the driving motor of the vehicle is still working, regardless of the state of the shifting motor.

3. Analysis of Shifting Time

On the basis of shifting process, the shifting time can be divided into 6 stages similarly. Here, the shifting time of gear engaging may be divided into two parts: the time determined by the driving motor, and the time determined by the shifting motor. Since the shifting motor is working throughout the shifting process, reduction of the shifting time depends mainly on the control of the driving motor. However, motor speed regulation is determined by inherent characteristics other than control of the driving motor. The shifting time of the power interruption/recovery process, as well as the synchronization time, are discussed in the following sections.

3.1 Power interruption and recovery time

Jerk is the rate of change of acceleration, and can be obtained by applying the vehicle dynamics equation when the gear is on the Gear:

$$j = \frac{da}{dt} = \left| \frac{1}{\delta m} \frac{d}{dt} \left(\frac{T_m i_g i_0}{r} - F_{load} \right) \right| \tag{1}$$

where j is the jerk, m is the vehicle mass, δ is the conversion coefficient of the rotating mass, T_m is the motor torque, i_g is the transmission ratio, i_0 is the final drive ratio, and r is the wheel radius.

Since the time of power interruption and recovery are short, it is assumed that the road conditions and vehicle speed remain constant in that short time interval. Hence, the vehicle jerk equation may be simplified as follows:

$$j = \frac{i_0}{\delta m r} \cdot i_g \cdot \left| \frac{dT_m}{dt} \right| \tag{2}$$

Supposing that the execution times for power interruption and recovery have a directly proportional variation with respect to shifting time, then $|dT_m/dt|$ is constant. Therefore, the shifting time of the power interruption and recovery can be obtained:

$$t = \frac{i_0}{\delta m r} \cdot \left(\frac{i_{g1} T_1 + i_{g2} T_2}{j} \right) \tag{3}$$

where i_{g1} and i_{g2} are the ratios of Gear 1 and Gear 2, respectively, T_1 is the target torque of Gear 1 when downshifting (or the torque at the beginning of Gear 1 when upshifting), and T_2 is the target torque of Gear 2 when downshifting (or the torque at the beginning of Gear 2 when upshifting). It can be concluded that the execution time of the power interruption and recovery depends on the changing gradient of the torque of driving motor, that directly determines the shifting jerk.

3.2 Synchronization time

According to Newton's second law, the dynamic model of the synchronizer can be defined as:

$$\Delta\omega = \int_0^t \dot{\omega}_V dt \tag{4}$$

$$J_V \dot{\omega}_V = \pm M_S - M_V \tag{5}$$

where $\Delta\omega$ is the rotational speed difference between the driving and driven part of the synchronizer, $\dot{\omega}_V$ is the angular speed of the synchronizer driven end, J_V is the equivalent moment of inertia of the synchronizer driven end, M_S is the friction moment (where "+" is used for upshifting, and "-" is used for downshifting), and M_V is the resisting moment of the synchronizer driven end.

According to Eq. (5), the vehicle jerk can be obtained as follows:

$$j = \frac{da}{dt} = \left| \frac{d}{dt} \left(\frac{(-M_s - M_V) r}{J_V i_0} \right) \right| \tag{6}$$

Using Eqs. (4), (5) and (6), the following equations can be obtained. The shifting time can be expressed as a symbolic function of the jerk.

$$\dot{\omega}_V = \frac{i_0}{r} \int_0^t j dt \tag{7}$$

$$\Delta\omega = \frac{i_0}{r} \int_0^t \left(\int_0^t j dt \right) dt \tag{8}$$

Through Eqs. (3) and (8), it is known that the shifting time is directly related to the shifting jerk. As the shifting time increases, the shifting jerk decreases. However, both shifting time and jerk are key indicators for shifting, and the control of the motor should be well weighed.

4. Analysis of Tooth Grinding

Synchronizer locking failure is the main cause of synchronizer tooth grinding. Synchronizer locking failure occurs when the synchronizer sleeve directly meshes with the target ring gear before entering into the correct locking position.

For a traditional AMT with a synchronizer installed on the output shaft, a lock ring can enter into the correct locking position in the downshifting process, while in the upshifting process, the lock ring must turn forward a tooth width relative to the synchronizer sleeve before entering into the correct locking position.[21] The same phenomenon occurs for AMT equipped on electric vehicles. Thus, for a pure electric vehicle with a two-speed AMT that has a synchronizer installed on the output shaft, synchronizer tooth grinding will not occur in the downshifting process, but will likely occur in the upshifting process.

In the upshifting process, after the synchronizer sleeve crosses the positioning slider clearance, the lock ring begins to turn relative to the

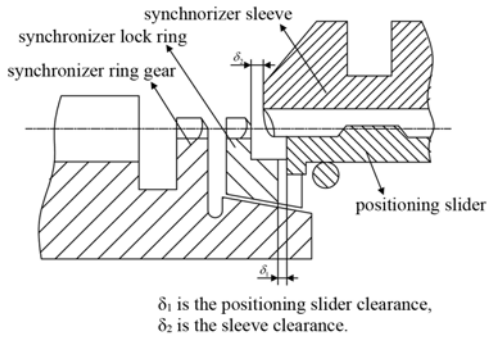

Fig. 5 Synchronizer axial clearance diagram for different parts

synchronizer sleeve, as shown in Fig. 5. To ensure that the lock ring enters into the correct locking position, it must turn forward a tooth width relative to the synchronizer sleeve before the synchronizer sleeve crosses the sleeve clearance. This may be defined as:

$$\frac{60}{\Delta nz} \le \frac{\delta_2 - \delta_1}{v_{jht}} \tag{9}$$

where v_{jht} is the axial movement speed of the synchronizer sleeve, Δn is the speed difference between the synchronizer driving and driven parts, z represents the lock ring tooth number, δ_1 is the positioning slider clearance, and δ_2 is the sleeve clearance, as shown in Fig. 5.

Using Eq. (9), the following equation is formulated:

$$v_{jht} \le \frac{(\delta_2 - \delta_1)\Delta nz}{60} \tag{10}$$

Obviously, Δn of the traditional AMT is larger, and the lock ring can quickly enter into the correct locking position since the allowed axial movement speed of the synchronizer sleeve is larger. However, Δn for the two-speed AMT of a pure electric vehicle is smaller since the speed of the driving motor can been adjusted quickly, thus limiting the allowed axial movement speed of the synchronizer sleeve. Therefore, the lock ring must slowly enter into the correct locking position, and this requirement diminishes the advantage of the motor speed regulation and extends the shifting time.

In conclusion, for AMT of pure electric vehicles, tooth grinding will generally not occur in the downshifting process and can be avoided in the upshifting process by extending the shifting time.

5. Shifting Process Control Strategy

To reduce the shifting time, decrease the vehicle jerk, and eliminate tooth grinding of the synchronizer, a shifting control strategy for pure electric vehicles is proposed based on parallel coordinated control of the driving and shifting motors. As shown in Fig. 6, the strategy mainly includes 3 types of algorithms: a power interruption and recovery control algorithm, a driving motor speed regulation control algorithm, and a gear disengaging/engaging control algorithm.

5.1 Power interruption and recovery control algorithm

In the power interruption and recovery processes, the core issue to be addressed is the first shifting jerk problem. According to the control strategy of the torque change rate of the driving motor, as long as the torque change rate of the driving motor satisfies the constraint conditions for jerk expressed in Eq. (3), the vehicle jerk during power interruption and recovery can be limited to the reference range.

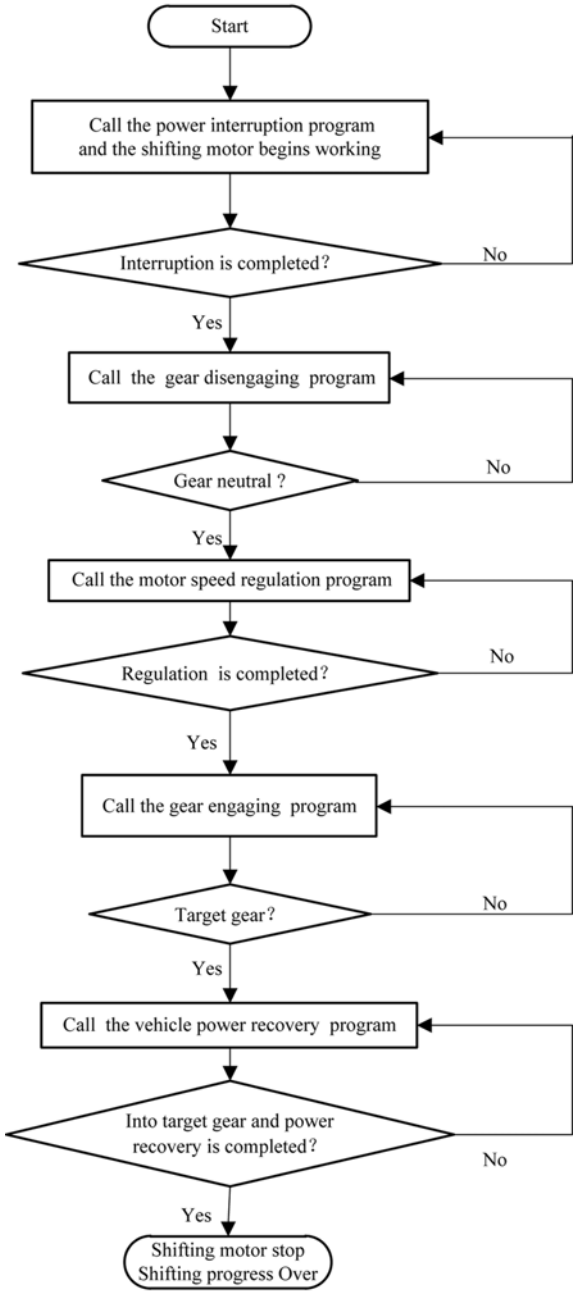

Fig. 6 Main process of the shifting control strategy

5.2 Driving motor speed regulation control algorithm

Motor speed regulation enables rapid reduction of the speed difference between the driving and driven synchronizer parts, thus reducing the synchronization load, prolonging synchronizer life, and reducing shifting time.

The core of the speed regulation control algorithm of the driving motor is a calculation of target speed. According to the downshifting

strategy, the speed of the lock ring should be lower than that of the synchronizer sleeve. The target speeds of the upshifting and downshifting speed regulations are expressed as follows, respectively:

$$n_{tar1} = i_1 n_0 - \Delta n_1 \tag{11}$$

$$n_{tar2} = i_2 n_0 - \Delta n_2 \tag{12}$$

where n_{tar1} is the target speed of the upshifting speed regulation, n_{tar2} is the target speed of the downshifting speed regulation, i_1 is the transmission ratio of Gear 1, i_2 is the transmission ratio of Gear 2, n_o is the output shaft speed, Δn_1 is the adjustment value of the speed regulation for the target speed of the driving motor during downshifting, and Δn_2 is the adjustment value of the speed regulation for the target speed of the driving motor during upshifting. The values of n_{tar1} and n_{tar2} can be optimized through dyno tests and prototype vehicle calibration.

5.3 Gear disengaging/engaging control algorithm

5.3.1 Gear disengaging

In the process of gear disengaging, the driving and shifting motors are concurrently controlled. The gearbox must be in the Gear neutral area before motor speed regulation can be completed. The process of gear engaging can be commenced after the motor speed regulation has been completed.

To ensure that the gearbox is in the Gear neutral area before the motor speed regulation is completed, the gear disengaging process is divided into two regions: the time optimal control region and the inertia region. The purpose of the time optimal control region is to ensure the rapidity of the gear disengaging process, while the purpose of the inertia region is to ensure that the gearbox is in the Gear neutral area before the motor speed regulation is completed.

If the motor speed regulation is completed in the time optimal control region, then the gear engaging process can begin immediately without the need for the inertia region.

(1) Control algorithm for the time optimal control region

Considering $\theta_h = B_2$ as the demarcation point between the time optimal control region and inertia region in the disengaging process of Gear 1, a mathematical model of the time optimal control region can be now be constructed through the following steps.

a) System state equation

The dynamic equation of the shifting actuator is expressed as follows:

$$J_h \ddot{\theta}_h = T_h i_h - T_f \tag{13}$$

where J_h is the equivalent rotational inertia of the shifting actuator on the shifting camshaft, θ_h is the angular displacement of the shifting camshaft, and T_f is the frictional moment of the shifting camshaft.

Let $\theta_h = x_1$, $\theta_h = x_2$. The system state equation may be expressed as follows:

$$\begin{cases} \dot{x}_1 = x_2 \\ \dot{x}_2 = \dfrac{T_h i_h - T_f}{J_h} \end{cases} \tag{14}$$

b) The boundary condition is $x_1(t_f) = B_2$, where t_f is the end time of the gear disengaging process.

c) The admissible control is $|T_h| \le T_{h\,max}$, where $T_{h\,max}$ is the maximum output torque of the shifting motor.

d) The performance indicator is t_f.

By solving the above optimal control model, the optimal control trajectories of the time optimal control region are expressed as follows:

$$T_h(t) = T_{h\,max}, \quad \theta_h \le B_2 \tag{15}$$

(2) Control algorithm for the inertia region

In the inertia region, driving motor speed regulation is not carried out, and the output torque of the shifting motor should be quickly reduced to zero. The shifting camshaft will approach the central or rear inertia region under the inertia moment, waiting for the completion of the motor speed regulation. In the inertia region, the gear engaging process can begin immediately if the speed regulation of the driving motor is completed.

5.3.2 Gear engaging

The control algorithm for gear engaging can be directly applied to the time optimal control algorithm. The optimal control trajectories of the gear engaging process of Gear 2 are expressed as follows:

$$T_h(t) = T_{h\,max}, \quad \theta_h \le M_4 + S_{kk} \tag{16}$$

where M_4 is the demarcation point of the $\theta_{2\text{-}N}$ transition and Gear 2 areas (as shown in Fig. 4), and S_{kk} is the minimum required stroke that guarantees the normal shifting of Gear 1 and Gear 2 (as shown in Fig. 4).

In the gear engaging process, another core issue to be addressed is the second type of shifting jerk. According to the control strategy, the torque change rate of the shifting motor must satisfy the jerk constraint conditions, which are expressed in Eq. (7).

Fig. 7 Pure electric vehicle with two-speed AMT

6. Experiments

To verify the shifting control strategy on the basis of the parallel coordination control method, a pure electric vehicle with a two-speed AMT is developed, as shown in Fig. 7. The vehicle and gearbox control units are replaced by D2P, and the control strategy is accomplished using the Motohawk rapid prototyping/production system. The test results are shown in Table 1.

Table 1 Shifting time

Shifting process diagram	Downshifting	Upshifting
Power interruption	0.15 s	0.15 s
Gear disengaging	0.1277 s	0.1360 s
Motor speed regulation	0.2587 s	0.3301 s
Synchronization and Gear engaging	0.3085 s	0.2103 s
Power recovery	0.15 s	0.15 s
Total time	0.9949 s	0.9764 s

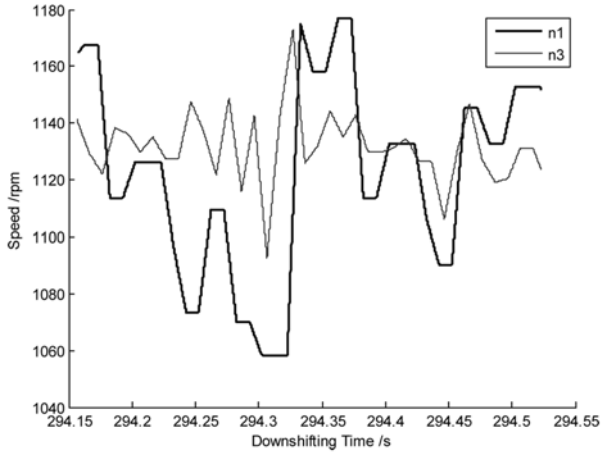

Fig. 8 Downshifting gear engaging

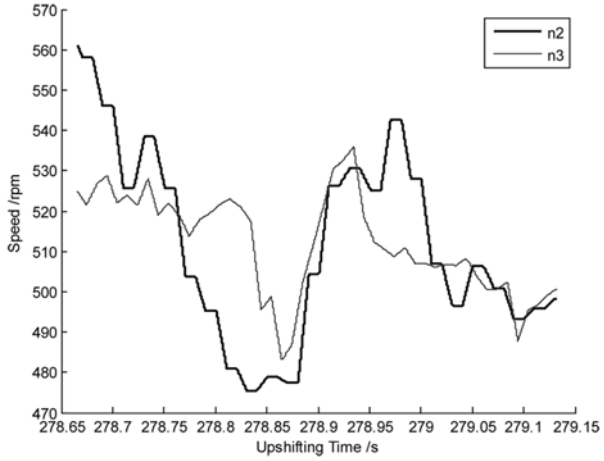

Fig. 9 Upshifting gear engaging

Because of matched driving motor constraints, the shifting vehicle speed is relatively fixed. So the results shown in Table 1 are universal for the selected vehicle. Of course, it should be noted that the time of 0.15 s in Table 1 does not mean that the power interruption and recovery require exactly 0.15 s. It means that the maximum permissible time for power interruption and recovery is 0.15 s. From Fig. 4, it is known that the parallel operation time of the driving and shifting motor is the sum of the time of power interruption and power recovery. It is up to 23.2% and 23.5% of the shifting time for upshifting and downshifting process of the serial controlling method respectively.

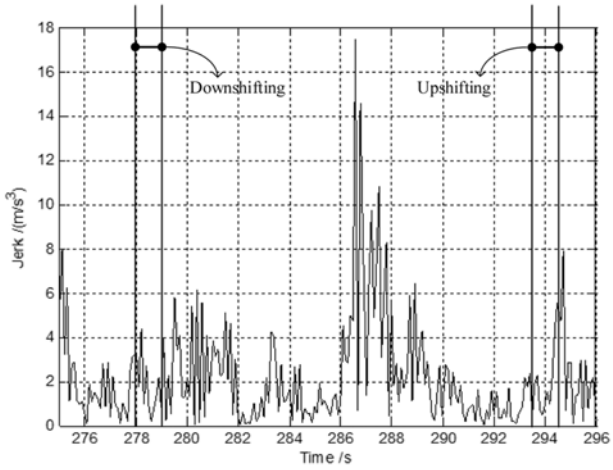

Fig. 10 Jerk data

The relationship between the lock ring speed of Gear 1 and the synchronizer sleeve speed is shown in Fig. 8. The relationship between the lock ring speed of Gear 2 and the synchronizer sleeve speed is shown in Fig. 9. From Figs. 8 and 9, it is known that the lock ring speed, n_2, of Gear 2 is lower than the synchronizer sleeve speed, n_3, in the upshifting process. However, in the downshifting process, the synchronizer sleeve speed, n_3, is higher than the lock ring speed, n_1, of Gear 1. This means that in the upshifting and downshifting processes, the synchronizer sleeve speed is always higher than the lock ring speed of the target Gear. Therefore, tooth grinding can be avoided both in the upshifting and downshifting process.

Based on Eq. (10) and the test data, the jerk results are shown in Fig. 10, including the stages of Gear 2, downshifting, Gear 1, and upshifting. From Fig. 10, it can be seen that during the processes of both downshifting and upshifting, the vehicle jerks are smaller than 10 m/s^3.

7. Conclusions

Shifting processes have been analyzed for a pure electric vehicle, equipped with a two-speed AMT without a clutch, to study the reasons for long shifting time and synchronizer tooth grinding during shifting processes. Dynamic models for vehicle and shift actuators have been constructed in order to analyze the shifting time and jerk. The geometry and kinematics of synchronizer parts have been studied in order to analyze the synchronizer tooth grinding during shifting processes. The analysis results show that: (1) shifting jerk is related to the torque variation rates of the driving and shifting motors. Shifting jerk can be decreased by decreasing the torque variation rates of the driving and shifting motors, but the shifting time will be extended; (2) tooth grinding will not generally occur in the downshifting process, but will likely occur in the upshifting process, and it can be avoided by extending the upshifting time.

Experimental results obtained from a real electric vehicle show that the shifting jerk and shifting time can be controlled within 10 m/s^3 and 1 s, respectively, with the proposed control strategy. Furthermore, there is no tooth grinding during shifting. It can be concluded that the proposed

control strategy can achieve reliable, smooth, and quick shifts.

As shifting time decreases, power performance increases. The following methods can be used to further reduce the total shifting time: 1) slightly increasing the power of the shifting motor; 2) improving the speed regulation of the driving motor; 3) replacing the single-cone synchronizer with a multi-cone synchronizer.

ACKNOWLEDGMENT

The authors would like to acknowledge the support and contribution from the State Key Lab of Mechanical Transmission, Chongqing University, China. This research was supported by the Key Project of Natural Science Foundation of CQ CSTC (Grant No.2011BA3019).

REFERENCES

1. Chan, C.-C., Bouscayrol, A., and Chen, K., "Electric, Hybrid, and Fuel-Cell Vehicles: Architectures and Modeling," IEEE Transactions on Vehicular Technology, Vol. 59, No. 2, pp. 589-598, 2010.
2. Nguyen, N. T., Ho, H. V., Hong, S.-T., and Bien, F., "Smart in-Wheel Generator using Adaptive DC-DC Converter for Rechargeable Batteries in Electric Vehicles," Int. J. Precis. Eng. Manfu., Vol. 15, No. 6, pp. 1009-1013, 2014.
3. Ehsani, M., Gao, Y., and Emadi, A., "Modern Electric, Hybrid Electric, and Fuel Cell Vehicles: Fundamentals, Theory, and Design," CRC Press, 2nd Ed., 2009.
4. Qin, D.-T., Zhou, B.-H., Hu, M.-H., HU, J.-J., and Wang, X., "Parameters Design of Powertrain System of Electric Vehicle with Two-Speed Gearbox," Journal of Chongqing University, Vol. 34, No. 1 pp. 1-6, 2011.
5. Xi, J.-Q., Xiong, G.-M., and Zhang, Y., "Application of Automatic Manual Transmission Technology in Pure Electric Bus," Proc. of IEEE Vehicle Power and Propulsion Conference, pp. 1-4, 2008.
6. Ren, Q., Crolla, D. A., and Morris, A., "Effect of Transmission Design on Electric Vehicle (EV) Performance," Proc. of IEEE Vehicle Power and Propulsion Conference, pp. 1260-1265, 2009.
7. Gao, B., Liang, Q., Xiang, Y., Guo, L., and Chen, H., "Gear Ratio Optimization and Shift Control of 2-Speed I-AMT in Electric Vehicle," Mechanical Systems and Signal Processing, Vols. 50-51, pp. 615-631, 2015.
8. Sohn, I. and Kim, B., "Comparison Benefit of E-Transmission for NEV," Int. J. Precis. Eng. Manuf., Vol. 15, No. 11, pp. 2465-2468, 2014.
9. Oh, J.-Y., Park, Y.-J., Lee, G.-H., and Song, C.-S., "Modeling and Validation of a Hydraulic Systems for an AMT," Int. J. Precis. Eng. Manuf., Vol. 13, No. 5, pp. 701-707, 2012.
10. Lucente, G., Montanari, M., and Rossi, C., "Modelling of an Automated Manual Transmission System," Mechatronics, Vol. 17, No. 2-3, pp. 73-91, 2007.
11. Heath, R. P. G. and Child, A. J., Zeroshift. "A Seamless Automated Manual Transmission (AMT) with no Torque Interrupt," SAE Technical Paper, No. 2007-01-1307, 2007.
12. Heath, R. P. G. and Child, A. J., "Zeroshift Automated Manual Transmission (AMT)," SAE Paper No. 2007-26-061, pp. 693-696, 2007.
13. Chen S, "Study on Parameter Matching and Intergrated Control Stragy for Pure Electrical Vehicle Driveline," Ph.D. Thesis, College of Mechanical Engineering, Chongqing University, 2013.
14. Zhang J, "Study on the Shifting Control without Clutch Operation of Electrical Controlled and Electronic Powered AMT," M.Sc. Thesis, Jilin University, 2007.
15. Chu M, "Study on the Electric Shifting of the AMT of Heavy-Duty Commercial Vehicle without the Disengagement of the Clutch," M.Sc. Thesis, Jilin University, 2007.
16. Wang S, "Engine Control on the Automatic Mechanical Transmission of Non-Clutch Operating," M.Sc. Thesis, Jilin University, 2007.
17. Kong, G., Zhong, Z., Yu, Z., and Chen, X., "Engine Control during Shifting Process of Automatic Mechanical Transmission Without Disengaging Clutch," Journal of Tongji University. Natural Science, Vol. 40, No. 2, pp. 267-271, 2012.
18. Wang, Y., Xi, J., and Chen, H., "A Study on the Mechanism and Counter Measures for Shift-Impact in AMT," Automotive Engineering, Vol. 31, No. 3, pp. 253-257, 2009.
19. Chen, Y., Liang, W., Xi, J., and Xu, C., "A Study on the Control Strategy for the Gear Shifting of AMT in a Electric Bus," Automotive Engineering, Vol. 33, No. 5, pp. 405-410, 2011.
20. Zhang Y, Qin D, Mi C, Guo J, "Two-Gear Automatic Gearbox of Electric Automobile," CN Patent, No. 102182798A, 2011.
21. Chen, J., "Automobile Construction (Lower Volumes)," Beijing: Machinery Industry Press, 2006.